EPJ Web of Conferences **107**, 10006 (2016)
DOI: 10.1051/epjconf/201610710006

Magic nuclei at explosive dynamo activity

V. N. Kondratyev[1,2]

[1]Physics Department, Taras Shevchenko National University of Kiev, 03022-UA Kiev, Ukraine
[2]Bogoliubov Laboratory of Theoretical Physics, JINR, 141980, Dubna, Russia

Abstract. Explosive nucleosynthesis at conditions of magnetorotational instabilities is considered for iron group nuclides by employing arguments of nuclear statistical equilibrium. Effects of ultra-strong nuclear magnetization are demonstrated to enhance the portion of titanium product. The results are corroborated with an excess of ^{44}Ti revealed from the Integral mission data.

1 Introduction

Energetic nuclear processes, e.g., core-collapse supernovae (SNe) [1, 2], heavy ion collisions [3] give rise to ultrastrong magnetic fields exceeding teratesla (TT). Magnetorotational instabilities (MRI) and/or dynamo action represent, plausibly, main respective mechanism. Then maximum magnetic field intensity at distances smaller than a radius r_0 from a center of the vortex dynamo process can be taken as a constant H_0. Strong magnetization of the MRI central region stabilizes magnetic fluxes Φ_0 also for field decaying components. Respectively, in conditions of a constant flux at radius $r > r_0$ the dependence of strength H on distance r can be represented as $H = \Phi_0/\pi r^2$. Comparable values for magnetic pressure gradients and gravitational force, i.e., $\mathrm{d}H^2(r)/\mathrm{d}r = 4H_0^2/b^2 r_a \sim 8\pi\,\mathrm{GM\,n}(R)/R^2$, determine the radius r_a relative to the MRI center corresponding to material irruption. Here, the gravitational constant G, the star mass M inside the bifurcation radius R is related to the matter density n(R) as $4\pi R^2\,\mathrm{n}(R) = -\mathrm{d}M/\mathrm{d}R$. Additional constraints on MRI parameters are given by shock wave energy E_s (see [1]) $H_0^2 r_0^2 \sim 8\,E_s / [L(2\text{-}b^{-1})]$, where L is total length of MRI areas, $b=(r_a/r_0)^2$. For typical SNe Type II values $R \sim 30$ km, $E_s \sim 10^{51.5}$ ergs at $H_0 \sim 3$ TT one obtains $r_0 \sim 10^{-0.5}$ km and $b \sim 10$. Nuclides produced in so strong fields (i.e., larger than 0.1 TT) contain an information on matter structure and explosion mechanisms (see [1,2,4-6] and refs. therein). In this contribution we analyze possibilities for using radionuclides to probe internal regions of respective sites.

2 Synthesis of ultramagnetized atomic nuclei

Abundances of iron group and nearby nuclides are described very successfully within nuclear statistical equilibrium (NSE) approach for over half a century, cf. [1,2,6,7], and for broader discussion of statistical models see [8] and refs. therein. At such conditions a nuclide abundance is determined mainly by its binding energy. The magnetic effects on the NSE were considered in [1,2,6] and refs. therein. Recall that at temperatures ($T \leq 10^{9.5}$ K) and field strengths (H $\geq$ 0.1 TT), the magnetic field dependence of relative output value $y = Y(H)/Y(0)$ is determined by a change in the binding energy of nuclei in a mgnetic field and can be written in the following form :

$$y = \exp\{\Delta B/kT\}. \qquad (1)$$

It is worthy to remind that NSE corresponds to a balance of strong and electromagnetic reactions with their inverse and meets β-equilibrium conditions with an equal number of protons and neutrons (i.e.Y_e = 0.5). In this situation predominantly symmetric nuclei (N=Z) are produced. Therefore, we consider as examples ^{56}Ni and ^{44}Ti. The choice of symmetric nuclei, double-magic and anti-magic at vanishing magnetization, gives a clear picture of magnetic effects in the formation of chemical elements and leads to fundamental conclusions about transmutation and synthesis of nuclei at ultra-strong magnetization.

2.1 Structure of magnetized nuclei

Within the mean field approximation the properties of nuclei are determined by single-particle energy levels filled up to the Fermi energy E_F, see [9]. The binding energy B can be written as $B = B_{\mathrm{LDM}} + C_n + C_p$, where C_i are the shell corrections for neutrons and protons, and the component B_{LDM} is calculated in semiclassical liquid drop model and varies only slightly in the magnetic field, according to the Bohr-van Leuven theorem, see [1,2].

Spin magnetization of Pauli type dominates for the neutron magnetic reactivity. Interaction of a field and the spin-magnetic moment corresponding to a spin projection

m_n on a field vector gives rise to a linear shift of level energy $\Delta = m_n g_n \omega_L$, where $\omega_L = \mu_n H$ with nucleon magneton μ_n, and g_n – neutron g–factor. Accordingly, the shell energy in a field H is modified as follows

$$C_n(H) = C_n^+(E_F + \Delta) + C_n^-(E_F - \Delta), \qquad (2)$$

where the indices + and – indicate a sign of the projection of spin magnetic moment on the field direction. This leads to a phase shift in dependence of the shell energy on number of neutrons N [1,2].

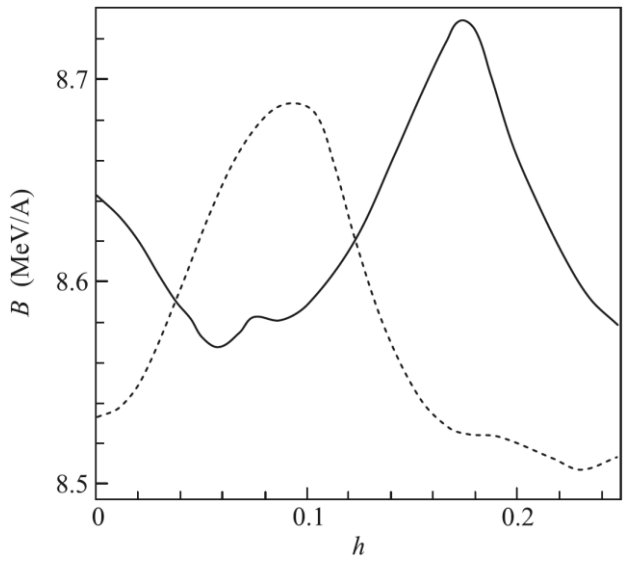

Fig. 1. Dependence of nuclear binding energy on magnetic field strength indicated by the parameter $h = \omega_L/\omega_0$. Results for ^{56}Ni – solid line and for ^{44}Ti – dotted line.

The proton magnetic response is represented by a superposition of the field interaction with spin and orbital magnetic moments. Great success in an understanding of many properties of stable nuclei of mass numbers $A \sim 10 - 100$ is associated with the Nilsson model (see, e.g., [9]) where the nuclear mean field is approximated by the harmonic oscillator with frequency $\omega_0 \approx 41/A^{1/3}$ MeV and the spin-orbit interaction, which leads to a splitting of energy levels $\eta_{so} \approx 0.12$ (in units ω_0). Magnetic field dependence of the total shell effect for neutron and proton contributions is shown in Fig. 1. We recall here similar consideration within the covariant density functional theory [10], which includes the interaction of the total magnetic moment of a nucleus with magnetic field, as well. As is evident from Fig. 1, at values $h < 0.07$, i.e., field strengths $H < 20$ TT, the binding energy shows nearly linear H dependence for considered nuclei, $B = B_0 + k_i H$ (MeV) with magnetic susceptibility parameters k_i depending on a nucleus $^A_N Z$. For ^{44}Ti the value of this parameter is positive k(Ti) ~ 0.3 MeV/TT, whereas for ^{56}Ni it becomes negative k(Ni) ~ - 0.3 MeV/TT. Evidently, for the anti-magic at zero field strength nucleus the shell energy always increases with the field H, and for the magic one – decreases, indicating positive and negative values of magnetic susceptibility κ_i, respectively.

2.2 MRI explosive nucleosynthesis

Let us consider an average relative yield of nucleosynthesis products over MRI region V (see Sec. 1)

$$\langle y \rangle = V^{-1} \int_V d^3 r \, y(H(\mathbf{r}))$$

Then using linear approximation for the binding energy (sect. 2.1), in a field H the average relative yield is written as follows:

$$\langle y \rangle = b^{-1}\left(\exp\{a\} + \int_1^b \exp\{a/x\}\,dx\right)$$
$$= \left(\exp\{a/b\} + \frac{a}{b}\left[\mathrm{Ei}(a) - \mathrm{Ei}(a/b)\right]\right), \qquad (3)$$

Where $a = k_i H_0/kT$ and the integral exponential function $\mathrm{Ei}(x) = \int_{-\infty}^{x} \frac{\exp\{t\}}{t}\mathrm{d}t$.

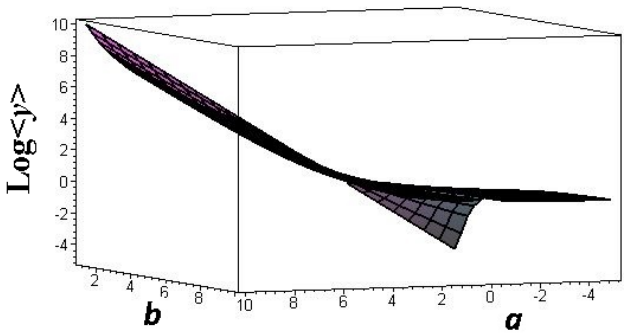

Fig. 2. Relative yield of nucleosynthesis products depending on parameters a and b.

In Fig. 2, one sees significant difference for magnetic field dependence of nuclide output, magic and anti-magic at vanishing field. For anti-magic nuclei and, therefore, increasing binding energy with the increase of the field strength (or positive magnetic susceptibility κ_i) relative volume of nucleosynthesis increases significantly with increasing a. At the same time, the relative production of magic nuclides, i.e., negative value a, is not substantially changed with increasing field. This behavior significantly differs from the case of a spatially uniform magnetization, see Fig. 2, which corresponds to the exponential dependence of $\langle y \rangle$ or $b = 1$ in Eq. (3). In this case the coefficients of suppression and enhancement are the same at the same absolute value of a. The presence of a diffusion layer corresponding to fade-out field strength with increasing r (or $b > 1$) in a real MRI region leads to substantial differences of relevant factors. Significant increase in a synthesis of anti-magic nuclei is accompanied by a slight change in mass volume of magic nuclides. Model predictions in an absence of magnetic effects (see Ref. [7]) give the mass of initially synthesized ^{44}Ti, M(Ti) ~ $10^{-5}\mathrm{M}_\odot$ (in solar masses $\mathrm{M}_\odot$). For realistic characteristics of Type II SNe explosion (see Sec. 1) enhancement factor $\langle y \rangle$(Ti)~ 30 – 300 corresponds to a mass M(Ti) ~ $10^{-3.5}$ - $10^{-2.5}$ $\mathrm{M}_\odot$.

3 Probing SN by radionuclides

As was shown above magnetic effects on the nuclear binding energy lead to an increase of the Ti portion in the explosive nucleosynthesis. Consequently, the characteristic lines of respective nuclei in spectra of astrophysical objects are considerably enhanced and become noticeable allowing for an analysis of synthesized elements. The radioactive decay chain ^{44}Ti → ^{44}Sc → ^{44}Ca gives rise to emission of lines with energies of 67.9 keV and 78.4 keV (from ^{44}Sc*) and 1157 keV (from ^{44}Ca*) of approximately equal intensity.

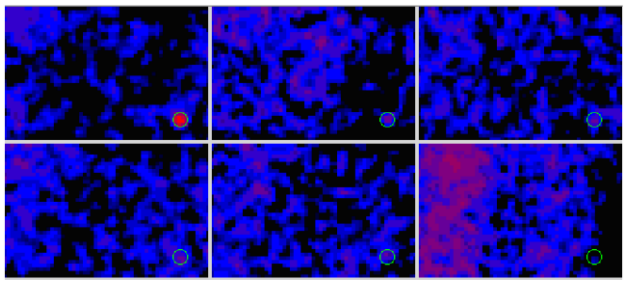

Fig. 3. (Color online) Direction (pixel number) dependence of the registered gamma-ray flux at different energy ranges. top: left - 20–50 keV, middle -50–67 keV, right - 67–70 keV, bottom: left - 70–77 keV; middle -77–82 keV, right – 82-100 keV; for the Cassiopeia region. SNR CAS A, (J2000) R.A. 350.86°, decl. 58.81°, is indicated by circle.

The respective image-mosaics from the Integral data (e.g., [1,2]) for the Cassiopeia region in various energy ranges of registered photons are presented in Fig. 3. The color (brightness) is proportional to the gamma-quanta flux: as larger the flux as lighter (brighter) the color of a pixel. As seen, the SNR CAS A gives the brightest spot for energies matching the ^{44}Sc lines.

Then the ^{44}Ti half-life, about 60 years, allows to determine this isotope initial mass in SN remnants. Table 1 shows the observational results for the total mass of ^{44}Ti nuclide synthesized in SNe explosions [6]. These values are significantly larger as compared to the model predictions in absence of magnetic effects (see Sec. 2). However, magnetic enhancement exceeds noticeably observational data. It is worthy to notice that not all the material ejected from the central part of a star is formed in MRI areas (see [1,2]). Accordingly, consideration of magnetic effects in nucleosynthesis when accounting for the realistic MRI structures and geometry can provide consistent understanding of SNe explosion mechanisms in detail.

Table 1. Bulk M(Ti) of nuclides ^{44}Ti (in solar masses $M_\odot$) initially synthesized in young SN – CAS A and SN1987A (see [6] and refs. therein).

SN	M(Ti) [10^{-4} $M_\odot$]
CAS A	$3.3^{+0.9}_{-0.7}$
SN1987A	3.1 ± 0.8

4 Conclusions

Nuclide abundances at conditions of the nuclear statistical equilibrium are investigated for developed explosive magneto-rotational instabilities and, respectively, the ultra-magnetized matter. For iron group nuclei the magnetic modification of nuclear structure shifts a maximum of the nucleosynthesis products towards smaller mass numbers approaching titanium. Magnetic effects in a nuclide production are favorable compared to observational Integral data and sensitive to the field geometry. Thermal effects can also affect structural and dynamical properties of atomic nuclei at high temperatures, see [11]. Finally, we notice that similar magnetic effects in atomic clusters [12] will also lead to a shift of electronic magic numbers and change the mass distribution.

Acknowledgements

This work is supported in part by scientific data center of Integral mission and SCOPES IZ73Z0_152485. The author (V.N.K.) thanks JINR (Dubna, Russia) for warm hospitality and financial support.

References

[1] V.N. Kondratyev, Phys. At. Nucl., **75**, 1368 (2012)
[2] V.N. Kondratyev, Eur. Phys. J. A **50,** 7 (2014)
[3] V. Voronyuk, V.D Toneev, W. Cassing, E. L. Bratkovskaya, V.P. Konchakovski, and S.A. Voloshin,. Phys. Rev. C **83**, 054911 (2011)
[4] V.N. Kondratyev, Phys. Rev. Lett. **88**, 221101 (2002)
[5] V.N. Kondratyev, Phys. Rev. C **69**, 038801 (2004)
[6] V.N. Kondratyev, Yu.V. Korovina, JETP Lett. **102**, 131 (2015)
[7] S.E. Woosley, A. Heger, T.A. Weaver, Rev. Mod. Phys. **74**, 1015 (2002)
[8] V.N. Kondratyev, Ph. Blanchard, H.O. Lutz, Eur. Phys. J. D **8**, 241 (2000)
[9] P. Ring, P. Schuck, *The Nuclear Many-Body Problem* (Berlin: Springer, 1980)
[10] D. Pena Arteaga, M. Grasso, E. Khan, P. Ring, Phys. Rev. C **84**, 045806 (2011)
[11] V.N. Kondratyev, M. Di Toro, Phys. Rev. C **53**, 2176 (1996)
[12] V.N. Kondratyev, H.O. Lutz, Eur. Phys. J. D **9**, 483 (1999)